Targeted Overexpression of TGF-α in the Corneal Epithelium of Adult Transgenic Mice Induces Changes in Anterior Segment Morphology and Activates Noncanonical Wnt Signaling

Yong Yuan,[*,1,4] *Lung-Kun Yeh,*[2,4] *Hongshan Liu,*[1] *Osamu Yamanaka,*[1] *William D. Hardie,*[3] *Winston W.-Y. Kao,*[1] *and Chia-Yang Liu*[*,1]

Purpose. Transforming growth factor-alpha (TGF-α) transduces its signal through the epidermal growth factor receptor and is essential for corneal epithelial homeostasis. Previous studies have demonstrated that overexpression of TGF-α in the developing eye leads to anterior segment dysgenesis. However, the underlying mechanisms remain unclear. Here we examined the effects of TGF-α overexpression on adult ocular surface homeostasis.

Methods. Binary Tet-On transgenic *Krt12*^{rtTA}*/tet-O-TGF-α* mice were subjected to doxycycline (Dox) induction to overexpress TGF-α in the corneal epithelium. Intraocular pressure (IOP) was measured by noninvasive tonometry. The enucleated eyes of the experimental mice were subjected to histopathology, immunohistochemistry, and biochemistry examination.

Results. Histologic and immunofluorescent examination showed that double-transgenic mice overexpressing TGF-α manifested peripheral anterior synechiae. Elevation of IOP, activation of glial cells, and loss of retinal ganglion cells were also observed. Quantitative real-time PCR revealed that the expressions of genes (*RXRα*, *PITX2*, and *FOXC1*) related to anterior segment dysgenesis were downregulated. Canonical Wnt signaling was suppressed, whereas noncanonical Wnt ligands (Wnt4 and Wnt5a) were upregulated. Increased myosin light chain phosphorylation suggested that noncanonical Wnt signaling is activated in affected eyes.

Conclusions. Overexpression of TGF-α in the corneal epithelium induces changes in anterior segment morphology. Corneal endothelial abnormalities are associated with the activation of the noncanonical Wnt and RhoA/ROCK signaling axis, indicating a potential application of RhoA/ROCK inhibitors as a therapeutic strategy for certain types of secondary angle-closure glaucoma. (*Invest Ophthalmol Vis Sci.* 2013;54:1829–1837) DOI:10.1167/iovs.12-11477

Transforming growth factor alpha (TGF-α) belongs to the epidermal growth factor (EGF) family of mitogens. Both TGF-α and EGF exert their biological activity by binding to the EGF receptor (EGFR). TGF-α was first discovered in the medium of virus-transformed cells.[1] TGF-α and EGFR also coexpress in many types of tumors, including breast carcinomas,[2] renal carcinomas,[3] and melanomas.[4] TGF-α was also found in wound fluid from skin graft donor site wounds.[5] However, the expression of TGF-α is not restricted to pathologic conditions. It also plays a pivotal role in embryonic development and adult homeostasis. TGF-α null mice display pronounced waviness of whiskers and fur, suggesting the role of TGF-α in hair follicle development. This animal also has subtle eye abnormalities. Some TGF-α null mice were born with their eyes partially open. The corneal epithelium appeared uniformly thinner and corneal inflammation was observed in affected eyes.[6,7] In addition to its role in hair and eye development, both EGF and TGF-α are also components of human tear fluid, indicating their role in corneal epithelial homeostasis.[8]

Although TGF-α is essential for normal eye development, excess TGF-α has detrimental effects on ocular surface morphogenesis during development. For example, it has been reported that α-crystallin promoter-driven human TGF-α overexpression in the lens manifested multiple eye defects including corneal opacities, cataracts, and microphthalmia due to altered cell fate of mesenchymal cells during embryonic eye development.[9] Interestingly, phenotypes of transgenic mice appeared associated with the level of TGF-α. For example, a milder phenotype was also noted in a similar transgenic mouse line expressing a lower level of TGF-α. In mildly affected transgenic eyes, the corneal endothelium did not differentiate properly and the iris directly attached to the cornea, manifesting a typical anterior segment dysgenesis (ASD) phenotype.[10] ASD is usually caused by mutation of genes critical for anterior segment morphogenesis, including *Pitx2*,[11] *FoxC1*,[12] *FoxE3*,[13] *BMP4*,[14] *Cyp1b1*,[15] *RXRα*,[16] and *DKK*.[17]

From the [1]Crawley Vision Research Laboratory, Department of Ophthalmology, College of Medicine, University of Cincinnati, Cincinnati, Ohio; the [2]Department of Ophthalmology, Chang-Gung Memorial Hospital, Chang-Gung University College of Medicine, Linko, Taiwan; and [3]Divisions of Pulmonary Biology and Pulmonary Medicine, Cincinnati Children's Hospital Medical Center, Cincinnati, Ohio.

[4]These authors contributed equally to the work presented here and should therefore be regarded as equivalent authors.

Supported in part by National Eye Institute/National Institutes of Health Grants EY21501 (C-YL) and EY013755 (WW-YK); Research to Prevent Blindness; Ohio Lions Eye Research Foundation; National Science Council (Taiwan) Grant 1012314B182A056MY3; and Grant CMRPG3A1291 from Chang-Gung Memorial Hospital, Linko (L-KY).

Submitted for publication December 12, 2012; accepted February 7, 2013.

Disclosure: **Y. Yuan**, None; **L.-K. Yeh**, None; **H. Liu**, None; **O. Yamanaka**, None; **W.D. Hardie**, None; **W.W.-Y. Kao**, None; **C.-Y. Liu**, None

*Each of the following is a corresponding author: Yong Yuan, Department of Ophthalmology, University of Cincinnati, 3230 Eden Avenue, Cincinnati, OH 45267; yuany@ucmail.uc.edu.

Chia-Yang Liu, Department of Ophthalmology, University of Cincinnati, 3230 Eden Avenue, Cincinnati, OH 45267; liucg@ucmail.uc.edu.

However, it is unclear whether TGF-α altered the expression pattern of those ASD genes during the anterior segment morphogenesis.

Here we report that excessive expression of TGF-α in the adult corneal epithelium causes anterior segment morphology changes associated with peripheral anterior synechiae and secondary angle-closure glaucoma. These observations resemble those of the human iridocorneal endothelial (ICE) syndrome. ICE syndrome is characterized by corneal endotheliopathy, secondary corneal edema, peripheral anterior synechiae, secondary glaucoma, and abnormalities of the iris stroma. Gene expression analysis revealed that several ASD genes (*PitX2*, *FoxC1*, *RXRα*, and *DDK*) were downregulated by TGF-α in the adult cornea. Canonical Wnt targets (*Lef1* and *Axin2*) were also downregulated, whereas noncanonical Wnt ligands (Wnt5a and Wnt4) were upregulated, suggesting the activation of noncanonical Wnt signaling.

Materials and Methods

Generation and Genotyping of *Krt12^{rtTA}/tet-O-TGF-α* Bitransgenic Mice

Krt12^{rtTA} knock-in mice[18] were crossed with *tet-O-TGF-α* mice[19] for the generation of *Krt12^{rtTA}/tet-O-TGF-α* double-transgenic mice, which overexpress TGF-α in the corneal epithelium upon induction with doxycycline (Dox). Transgenic mice were identified by polymerase chain reaction (PCR) using the following primers: Forward *Krt12-1* (primer 1): 5′-GTG TGT GCC TGC CAT CCC ATC-3′, *Neo781-803* (primer 2): 5′-CGC CTT CTT GAC GAG TTC TTC TG-3′ for knock-in allele, *Krt12-1* primer, and reverse *Krt12-2* (primer 3): 5′-GAT CTG GGG TTG CAA TGA AGAC-3′ for wild-type allele. Cytomegalovirus (CMV) minimum promoter forward primer, 5′-GTC AGA TCG CCT GGA GAC GCC-3′, reverse primer in hTGF-α, 5′-CGT GGT CCG CTG ATT TCT TCT CTA-3′ for detecting the *tet-O-TGF-α* transgene.

Dox induction was administered through Dox chow (1 g/kg) without restriction. Experimental transgenic mice induced with Dox from postnatal day 20 (P20) to different ages including P22 (Dox2), P25 (Dox5), and up to P40 (Dox20). The eyes were enucleated and subjected to histologic analysis and immunocytochemistry. Animals were housed under pathogen-free conditions in accordance with institutional guidelines. Animal care and use conformed to the ARVO Statement for the Use of Animals in Ophthalmic and Vision Research. All animal protocols were approved by the Institutional Animal Care and Use Committee of the University of Cincinnati.

Immunohistologic and Western Blotting Analysis

The following antibodies were used in the study: red-fluorescent Alexa Fluor 594 anti–glial fibrillary acidic protein (GFAP) monoclonal antibody (A-21295; Invitrogen, Carlsbad, CA), anti-N-cadherin antibody (04-1126; Millipore, Billerica, MA), anti–proliferating cell nuclear antigen (PCNA) antibody (ab2426; Abcam, Cambridge, UK), antiphospho-myosin light chain 2 (Ser19) antibody (3675; Cell Signaling Technology, Inc., Beverly, MA). Secondary Alexa488, Alexa555-labeled antibodies were obtained commercially (Molecular Probes/Life Technologies Corp., Carlsbad, CA). Immunohistologic analysis was performed to determine the consequences of excess TGF-α in corneas of *Krt12^{rtTA}/tet-O-TGF-α* mice and control uninduced littermates. Excised eyes were fixed in 4% paraformaldehyde in 0.1 M phosphate buffer (PB; pH 7.4) at 4°C overnight and paraffin embedded. Sections (5 μm) were then mounted on microscope slides (Superfrost slides; Fisher Scientific, Pittsburgh, PA). The sections were deparaffinized and hydrated in a graded ethanol series (95%, 75% ethanol, and PBS for 3 minutes each). Antigen retrieval was performed by boiling the slides in citrate buffer for 10 minutes. All incubations were performed at room temperature. Sections for immunofluorescence analysis were mounted (SlowFade Light Antifade Kit; Molecular Probes, Eugene, OR) in the presence of 4′,6-diamidino-2-phenylindole, observed with an epifluorescence microscope (Axioscop2; Carl Zeiss, München-Hallbergmoos, Germany), and were photographed with a digital camera system (Axiocam; Carl Zeiss GmbH, Oberkochen, Germany).

Western blot was performed to verify the expression of TGF-α in experimental animals. Mice were euthanized and the corneas were immediately dissected and placed in 400 μL in PBS containing 3% CHAPS and protease inhibitors. The corneas were then homogenized with a cell-disrupting reagent (FastPrep Cell Disrupter; BIO 101, Vista, CA). Following homogenization and centrifugation, supernatants were collected and protein concentration was determined by the absorbance at 280 nm using a spectrophotometer (Nanodrop 2000; Nano Drop Technologies, Wilmington, DE). An equal amount of protein (40 μg) was loaded into each well of the 4%–12% Bis-Tris gel with MES SDS running buffer (Invitrogen) and Western blotting was performed using rabbit anti-TGF-α antibody (ab9585; Abcam); normalization was done with anti-actin antibody (Sigma-Aldrich, St. Louis, MO).

Measurement of Intraocular Pressure and Endothelial Morphology

IOP was measured in the morning between 10 and 11 AM, at each time point of day 0, day 5, day 10, and day 20 after induction by using a tonometer (TonoLab; Colonial Medical Supply, Franconia, NH). Two groups of mice, 4 to 6 weeks of age, were anesthetized by intraperitoneal injection of ketamine hydrochloride (0.1 mg/gm body weight) and xylazine (0.02 mg/gm body weight). The tonometer (TonoLab; Colonial Medical Supply) was applied to the right cornea of each mouse for measuring IOP. All data (IOP measurements) are presented as means ± SD. Statistical analysis was performed by using the Student's *t*-test to assess the statistical significance. Values of $P < 0.05$ were considered statistically significant.

In vivo analysis of the corneal endothelium was performed with a retinal tomograph (Heidelberg Retinal Tomograph–HRT II Rostock Cornea Module; Heidelberg Engineering GmbH, Heidelberg, Germany) according to the manufacturer's instructions. Briefly, a drop of disappearing preservative (GenTeal Gel; Novartis Pharmaceuticals Corp., East Hanover, NJ) was applied to the tip of the HRT-II objective as immersion fluid. Subsequently, a series of images were collected to cover the whole corneal thickness as a continuous *z*-axis scan at 1- to 3-μm increments, starting from the corneal epithelium and ending at the corneal endothelium.

RNA Extraction and qRT-PCR

Total RNAs were isolated from eight pooled corneas by rapid separation of total RNA (FastRNA Pro Green Kit using a FastPrep Instrument; MP Biomedicals, Solon, OH). In all, 5 μg of total RNA were reverse transcribed using a synthesis kit for qRT-PCR (Maxima First Strand cDNA Synthesis Kit; Fermentas GmbH, St. Leon-Rot, Germany). PCR reactions were performed on a real-time PCR system (CFX96 using CFX Manager Software; Bio-Rad Laboratories, Hercules, CA). Primer sequences used in the study are listed in the Table. Glyceraldehyde-3-phosphate dehydrogenase (GAPDH) was used as the housekeeping gene to normalize expression levels.

Results

Overexpression of TGF-α in Adult Corneal Epithelium Causes Corneal Opacification and Neovascularization

Bitransgenic mice *Krt12^{rtTA}/tet-O-TGF-α* specifically overexpress TGF-α in corneal epithelial cells upon Dox induction (Fig. 1A). Without Dox induction, the *Krt12^{rtTA}/tet-O-TGF-α* double-transgenic mice exhibited no anomaly in the cornea or other

TABLE. Primer Sequences Used in qRT-PCR

Gene Name	Accession Number	Forward Primer	Reverse Primer	Start	End
Foxc1	NM_008592.2	ATTCAGCTCACCAGCATCAG	CAAGACGAATGAGCAGGAAA	2375	2583
Foxe3	NM_015758.2	ACTCATACATCGCGCTCATT	AAACAGTCGTTGAGGGTGAG	200	365
Lmx1b	NM_010725.2	GGTTTCAGAACCAAAGAGCA	CGATATCGTGGAAGATGGAG	728	988
Pax6	NM_001244202.1	AGAGTTCTTCGCAACCTG	CATCTGAGCTTCATCCGAGT	1214	1448
Pitx2	NM_001042504.1	ACTGGAAGCAAAGCAGCACT	AGTCTTTCTGGGGCAGAGTT	966	1128
Rxra	NM_011305.3	CTCTAAGGGGCTCTCAAACC	GAAGAAGAACAGGTGCTCCA	1384	1564
Dkk1	NM_010051.3	CGCTGCATGAGGCACGCTAT	GGCGGCGTTGTGGTCATTAC	484	624
Dkk2	NM_020265.4	AAGGCCACACTCCAAGATGC	AGAAGTGGCGAGCACAACAA	1239	1340
Dkk3	NM_015814.2	AGTGCCGTGGAGGAGATGGA	GGTGCACATGGACTGTGTTA	314	452
Axin1	NM_001159598.1	CCCCCATACAGGATCCGTAA	GGTACCCGCCCATTGACTT	1467	1538
Axin2	NM_015732.4	GCCGACCTCAAGTGCAAACTC	GGCTGGTGCAAAGACATAGCC	1058	1231
Lef1	NM_010703.3	AGACACCCTCCAGCTCCTGA	CCTGAATCCACCCGTGATG	1551	1673
Tcf4	NM_001142923.1	GTTTGGAAGAAGCGGCCAAG	GGTGAAGTGTTCATTGCTGTACTG	777	1100
Wnt11	NM_009519.2	TGCTTGACCTGGAGAGAGGT	AGCCCGTAGCTGAGGTTGT	565	757
Wnt4	NM_009523.2	CGAGGAGTGCCAATACCAGT	GTCACAGCCACACTTCTCCA	270	462
Wnt5a	NM_001256224.1	ACACAACAATGAAGCAGGCCGTAG	GGAGTTGAAGCGGCTGTTGACC	673	893
Wnt1	NM_021279.4	ATCCATCTCTCCCACCTCCT	AGCAACCTCCTTTCCCACTT	1558	1959
Wnt10a	NM_009518.2	GCGCTCCTGTTCTTCCTACT	ATGCCCTGGATAGCAGAGG	222	418
Wnt7a	NM_009527.3	GACAAATACAACGAGGCCGT	GGCTGTCTTATTGCAGGCTC	948	1154
Wnt8b	NM_011720.3	CCAGAGTTCCGGGAGGTAG	GAGATGGAGCGGAAGGTGT	724	854
Wnt9a	NM_139298.2	CACAACAACCTCGTGGGTGTGAAG	GGGAGAGTCGTCCAGGTGTACAAG	635	931
Gapdh	NM_008084.2	TGGCAAAGTGGAGATTGTTGCC	AAGATGGTGATGGGCTTCCCG	119	274

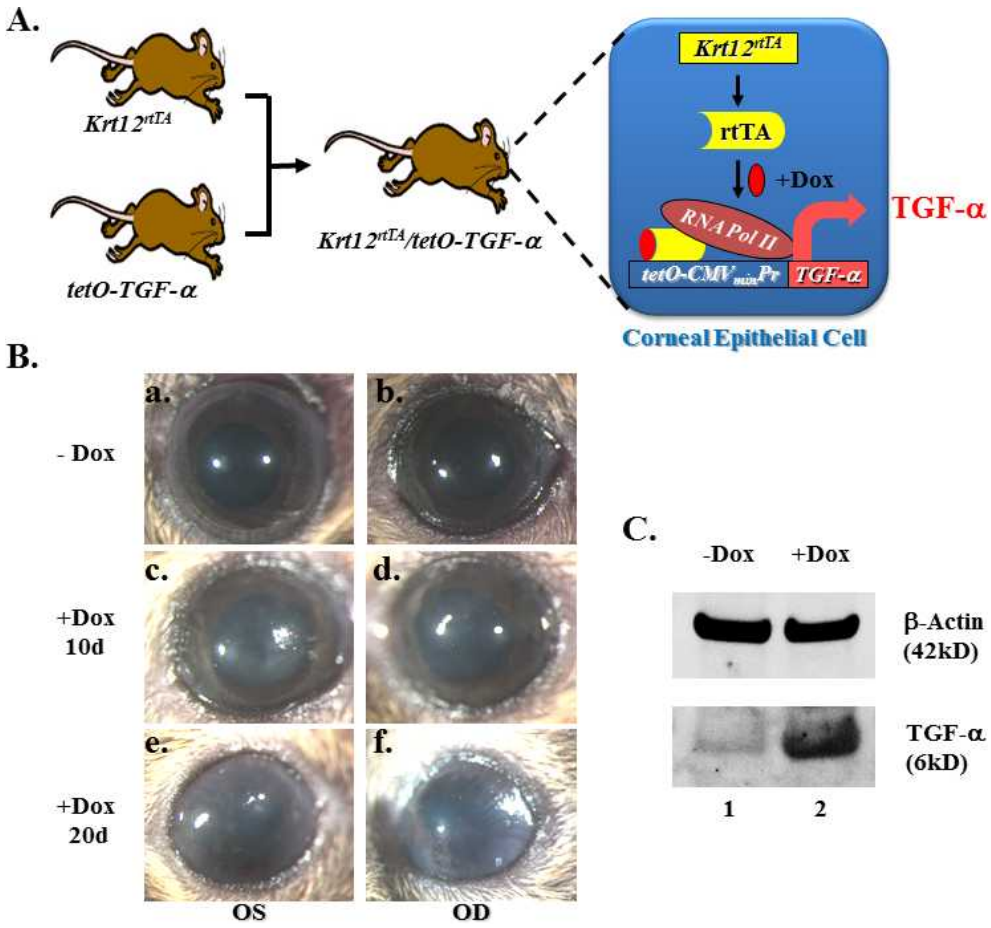

FIGURE 1. Overexpression of TGF-α in adult corneal epithelium caused corneal opacification and neovascularization. (**A**) Diagram shows the generation of bitransgenic mouse strain *Krt12*^{rtTA}*/tet-O-TGF-α*. TGF-α overexpression in the corneal epithelial cells occurs upon Dox treatment. (**B**) Bitransgenic mouse eyes have clear cornea before Dox induction (–Dox, in [**Ba**, **Bb**]), but exhibited corneal opacity when treated with Dox for 10 days (+Dox 10d, in [**Bc**, **Bd**]). Noted blood vessels started growing toward the central cornea after 20 days of induction (+Dox 20d, in [**Be**, **Bf**]). (**C**) Western blotting revealed that the active form TGF-α (6 kDa) level increased dramatically after 10 days of Dox induction. β-Actin served as the loading control. OD, oculus dexter (right eye); OS, oculus sinister (left eye).

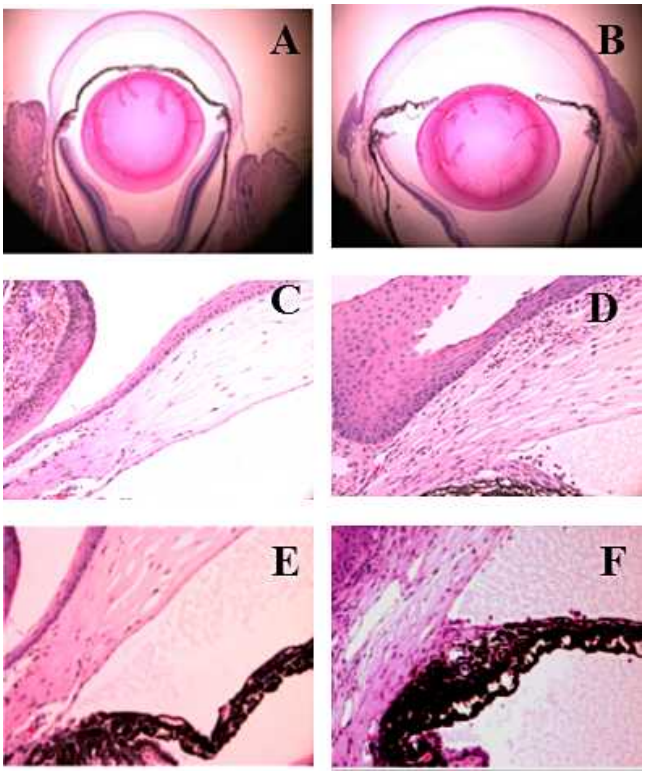

Figure 2. Overexpression of TGF-α in adult corneal epithelium caused limbal epithelial hyperplasia and iridocorneal angle closure. There were two major differences between control (**A**) and TGF-α–expressing eyes (**B**) as revealed by H&E staining, the thickness of limbal epithelium and anatomic configuration of the iris (**B**). The thickness of the limbal epithelium was dramatically increased and the iris positioned in a flat plane in experimental eyes. High magnification showed massive limbal epithelial tissue in the experimental eye (**D**) as compared with the control eye (**C**). Control eye (**E**) had a normal iridocorneal angle, whereas extra tissue was clearly visible in the closed angle of the TGF-α–expressing eye (**F**).

tissues and survived normally in the vivarium. After 10 days of Dox induction, the cornea became opaque (Figs. 1Bc, 1Bd). New blood vessels emerged and grew toward the central cornea after 20 days of induction (Figs. 1Be, 1Bf). The expression level of TGF-α was significantly increased after 10 days of Dox induction, as revealed by Western blot analysis (Fig. 1C).

Histologic examination of the globe revealed an increase of limbal epithelium cell layers following 20 days of TGF-α stimulation (Fig. 2B). Gross morphologic analysis revealed a flat iris plane in experimental mice (Fig. 2B). Detailed examination of limbus and iridocorneal angle revealed the hyperproliferative limbal epithelial cells (Fig. 2D) and the presence of extra tissue in the closed iridocorneal angle (Fig. 2F).

TGF-α Elicited Secondary Angle-Closure Glaucoma

The observation of an altered iridocorneal angle caused by excess TGF-α led us to believe that this may lead to an increase in IOP, which started to increase 5 days after Dox induction. After 20 days of induction, the IOP doubled (Fig. 3A). In control mice, the retinal ganglion cell layer consisted of one to two layers of well-organized cells (Fig. 3B). After 20 days of TGF-α expression, a single layer of sparse ganglion cells was evident, suggesting the loss of retinal ganglion cells (Fig. 3C). GFAP, a marker of activated glial cells in response to pathologic insults, has been reported in retinal detachment, mechanical injury, retinal degeneration, and glaucoma.[20] In control eyes, only the inner layer of the retina (nerve fiber and ganglion cell layers) was weakly positive (Fig. 3D). After 2 days of TGF-α expression, weak positive signals began to show up in all layers of the retina (Fig. 3E). After 5 days of induction, strong positive signals were found in elongated cells extending from the inner retinal cell layer to the outer cell layer of photoreceptors (Fig. 3F). Similar but intensified signals were observed after 20 days of induction (Fig. 3G).

Endothelial Abnormality Is Associated with Noncanonical Wnt Signaling

N-Cadherin is an endothelial cell marker, and N-cadherin staining in the control eye was positive on the endothelial side, whereas cells at the angle and anterior iris were negative (Fig. 4A). A similar N-cadherin pattern kept unchanged after 5 days of Dox induction (Figs. 4B, 4C). After 20 days of the induction, N-cadherin–positive cells were found on both sides of the angle (Fig. 4D). PCNA staining was used to verify endothelial cell proliferation. In control eyes, PCNA-positive cells were restricted to the basal cells of the corneal epithelium (Fig. 4E). Upon TGF-α expression, PCNA epithelial staining intensified and decorated several layers of the epithelium. PCNA-positive cells were also present in the limbal stroma (Fig. 4F). After 5 days of Dox induction, positive, albeit weak, PCNA cells can be found in the corneal endothelium (Fig. 4G). After 20 days of Dox induction, PCNA-positive cells were found on both sides of the angle, with a stronger fluorescence signal on the peripheral anterior iris (Fig. 4H). Excess TGF-α changed cell morphology and reduced cell density of the corneal endothelium. Live images of the corneal endothelium were taken by HRT II Rostock cornea module (Carl Zeiss). Corneal endothelial cells mostly exhibited a hexagonal shape in untreated mice (Fig. 4I), but assumed diffuse abnormality of the corneal endothelial cells with pleomorphism in size and shape. The loss of clear hexagonal cell shape in the treated mice was also evident (Fig. 4J). In addition, the endothelial cell density of Dox-treated mice was reduced by 19.4% as compared with the nontreated mice (from 2736 ± 28 cells/mm^2 to 2204 ± 43 cells/mm^2). These phenomena recapitulate some features of the ICE syndrome.

To find out the molecular mechanism underlying the endothelial abnormality, we took another approach. It was previously demonstrated that overexpression of TGF-α in the lens during embryonic development causes anterior segment dysgenesis (ASD) of the eye.[10] We analyzed the expression of ASD genes in the corneas of our adult TGF-α–expressing mice. As expected, the expressions of several ASD genes were downregulated by TGF-α induction as shown by qRT-PCR, including: *RXRα*, *Pitx2*, *FoxC1*, and *DKK3* (Fig. 5A). It has been proposed that retinoic acid, *Pitx2*/*FoxC1*, and *DKK* play critical roles during anterior segment development by suppressing canonical Wnt signaling.[21] So we analyzed the expression of canonical Wnt targets. We chose four genes (*Axin1*, *Axin2*, *Lef1*, and *TCF4*) in Wnt/beta-catenin signaling, two of which (*Axin2* and *Lef1*) were previously reported as targets of Wnt signaling.[22,23] Because we observed a downregulation of Wnt signaling suppressors, we expected *Axin2* and *Lef1* to be upregulated. To our surprise, they were downregulated (Fig. 5B), suggesting the suppression of canonical Wnt signaling. Next, we analyzed the expression of Wnt ligands. Only the Wnt ligands with cycle threshold (Ct) value below 30 are shown. Among them, Wnt4, Wnt5a, and Wnt9a (Wnt14) were upregulated more than 2-fold (Fig. 5C). All of them are noncanonical Wnt ligands. Another noncanonical Wnt ligand (Wnt11) was downregulated. Because Wnt5a can activate RhoA, leading to increased phosphoryla-

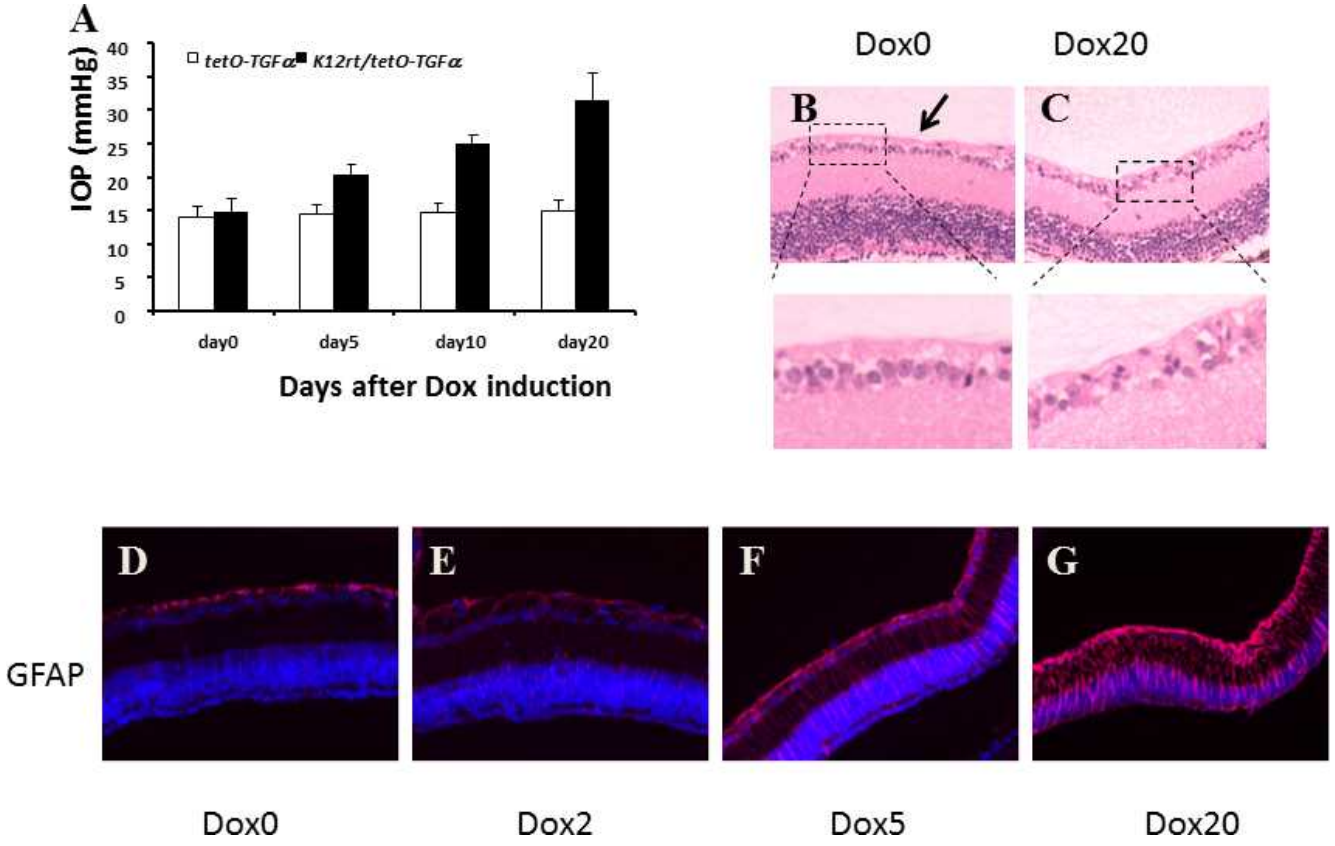

Figure 3. TGF-α expression led to elevated IOP, Müller glial cell activation, and retinal ganglion cell loss (**A**), IOP was measured in single- and double-transgenic mice before Dox induction and recorded as day 0. After 5, 10, and 20 days of Dox induction, IOP values of single-transgenic mice were steady during the course of induction, whereas IOP values of double-transgenic mice increased steadily and significantly. The data were collected from four mice of each group. TGF-α expression led to retinal ganglion cell loss (**B**, **C**). In control mice (**B**), the retinal ganglion cell layer consisted of one to two layers of well-organized cells (*arrow*). After 20 days of TGF-α expression, a single layer of sparse ganglion cells was evident (**C**). Immunoreactivity for GFAP in the retina revealed progressive activation of Müller glial cells by TGF-α expression (**D**–**G**). Before Dox induction (**D**), GFAP was localized in the nerve fibers and ganglion cell layer. After 2 days of induction (**E**), GFAP-positive signals were visible in all layers of the retina. After 5 days of induction (**F**), strong immunoreactivity was found in nerve fiber, ganglion cell layers, and in elongated cells extending across the whole section of the retina. The signal intensified after 20 days of induction (**G**).

tion of myosin light chain (MLC), we wanted to see if the phosphorylated-MLC pattern was altered in our samples. After 2 days of induction, a strong phospho-MLC signal started showing up in the angle region, possibly in the trabecular meshwork (Fig. 5E). After 5 days of induction, both corneal endothelium and trabecular meshwork were heavily decorated with MLC-P (Fig. 5F). After 20 days of induction, the closed angle and both sides of the angle were positive (Fig. 5G). The downregulation of canonical Wnt targets and upregulation of noncanonical Wnt ligands and increased MLC phosphorylation suggested the activation of noncanonical Wnt signaling.

Discussion

Here we report a mouse model of secondary angle-closure glaucoma elicited by inducible expression of TGF-α in the corneal epithelium. This model shares some common features with DBA/2J mice.[24] Both mice develop a progressive form of secondary angle-closure glaucoma that is associated with anterior synechiae formation, elevated IOP, and loss of retinal ganglion cells. The presence of endothelium on the surface of the trabecular meshwork and the peripheral iris in both mice closely resembles characteristics of the ICE syndrome in humans.

ICE was first proposed by Yanoff[25] to unify common features of three different diseases: Iris–nevus syndrome, Chandler's syndrome, and essential iris atrophy. The fundamental abnormality among the diseases is the presence of the corneal endothelium on the peripheral iris. The presence of endothelium and abnormal basement membrane on the surface of the trabecular meshwork and peripheral iris lead to a decrease in outflow of aqueous humor and elevation of IOP. We observed some similarities between our mouse model and ICE syndrome in terms of endothelial changes. After 20 days of TGF-α expression, corneal endothelial cells extended over the iridocorneal angle, covering the surface of the peripheral iris. Elevation in IOP and retinal glial cell activation (GFAP staining) were confirmed in our mouse model.[26] After 2 days of induction, we found increased staining of phosphorylated MLC in the corneal endothelium and trabecular meshwork, suggesting the activation of RhoA,[27] which has also been demonstrated in the glaucomatous trabecular meshwork.[28] Increased IOP was observed as early as 5 days after induction. At this time point, only partial peripheral anterior synechiae were observed. This suggests that increased phosphorylation of MLC in the trabecular meshwork may be responsible for IOP elevation and the endothelization of the anterior iris is a later event.

Even clinical observations clearly showed endothelial cells on the anterior iris[29]; however, we do not know if it is due to

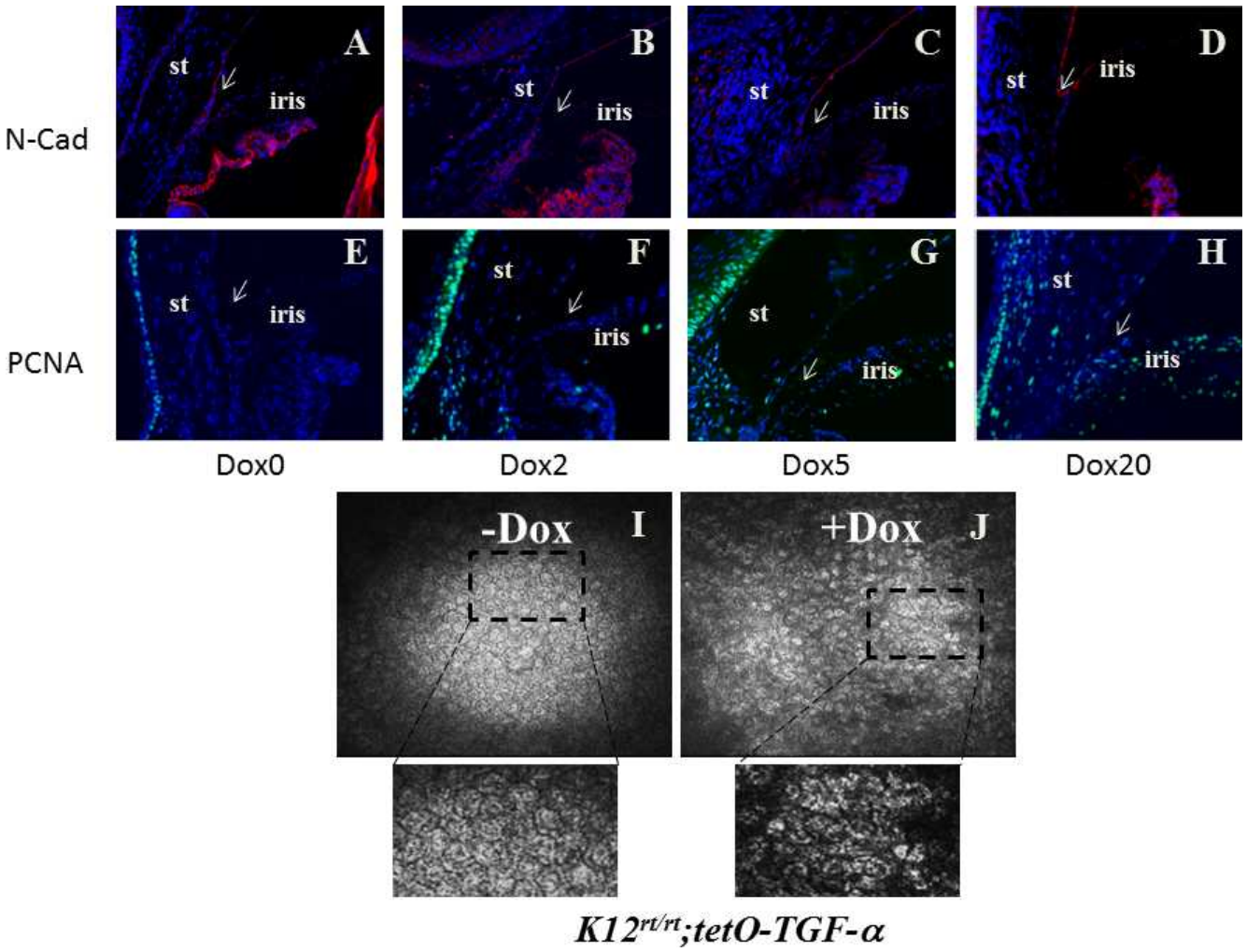

Figure 4. TGF-α expression led to corneal endothelial abnormality. N-Cadherin is the marker to track corneal endothelium. After 2 days of induction, corneal endothelium and trabecular meshwork were positive (**A**, **B**). After 5 days of induction, only the endothelium was positive (**C**). After 20 days of induction, N-cadherin–positive cells were also visible on the anterior iris, forming a continuous cell layer blocking the iridocorneal angle (*arrow* in [**D**]). Cell proliferation marker PCNA was positive in the corneal epithelium (**E**–**H**). Before induction, it was negative on corneal stroma and iris (**E**). Two to 5 days after induction, positive cells were also visible in the stroma (**F**, **G**). Twenty days after induction, both the corneal endothelium and peripheral iris were positive (**H**). Excess TGF-α changed the cell morphology and reduced cell density of the corneal endothelium. Live images of the corneal endothelium were taken by HRT II Rostock cornea module. Corneal endothelial cells mostly exhibited a hexagonal shape in untreated mice (**I**), but assumed diffuse abnormality with pleomorphism in size and shape in the treated mice (**J**). In addition, the endothelial cell density of Dox-treated mice reduced by 19.4% as compared with the nontreated mice (from 2736 ± 28 cells/mm^2 to 2204 ± 43 cells/mm^2).

cell proliferation or/and to migration. Positive PCNA staining was observed in the experimental endothelium, whereas control endothelium remained negative, suggesting the role of endothelial cell proliferation. Notwithstanding, HRT II live image data suggested that the cell migration also occurred in effected eyes, because reduced cell density and loss of hexagonal cell shape were observed. So, which signaling pathways are responsible for the proliferation and migration of corneal endothelial cells? Corneal endothelial cells in culture are able to enter and complete the cell cycle upon loss of cell–cell contact with EDTA treatment and the presence of mitogens.[30] Under this condition, canonical Wnt signaling is activated and cells lose the normal phenotype due to endothelial–mesenchymal transition.[31] Corneal endothelial cells can also proliferate while keeping cell–cell contact. Edward et al.[32] reported corneal endothelial cell proliferation in neurofibromatosis type 1 (NF-1) patients whose corneal endothelium expressed no functional neurofibromin 1 (NF1) protein. They reported similar features of anterior segment endothelization in NF-1 patients to those seen with ICE syndrome. Zhu et al.[31] reported that activation of RhoA/ROCK signaling by knocking down p120 catenin was required for corneal endothelial cell proliferation without disrupting the adherens junction. Because loss of NF1 has been reported to activate RhoA-ROCK signaling,[33] the pathways converge on RhoA/ROCK signaling. We also observed increased MLC-phosphorylation in our mouse model, which is a downstream target of RhoA/ROCK signaling, suggesting RhoA/ROCK activation in our model. If RhoA/ROCK activation is a prerequisite for corneal endothelial cell proliferation, RhoA/ROCK inhibitors, which have been demonstrated to lower the IOP through relaxing trabecular meshwork cells,[34] could potentially be used to treat ICE syndrome or prevent endothelial cells from regrowing over the angle after filtering surgery.

Although RhoA/ROCK signaling may be important for corneal endothelial homeostasis, little is known regarding the underlying mechanism(s) or key upstream regulatory genes/

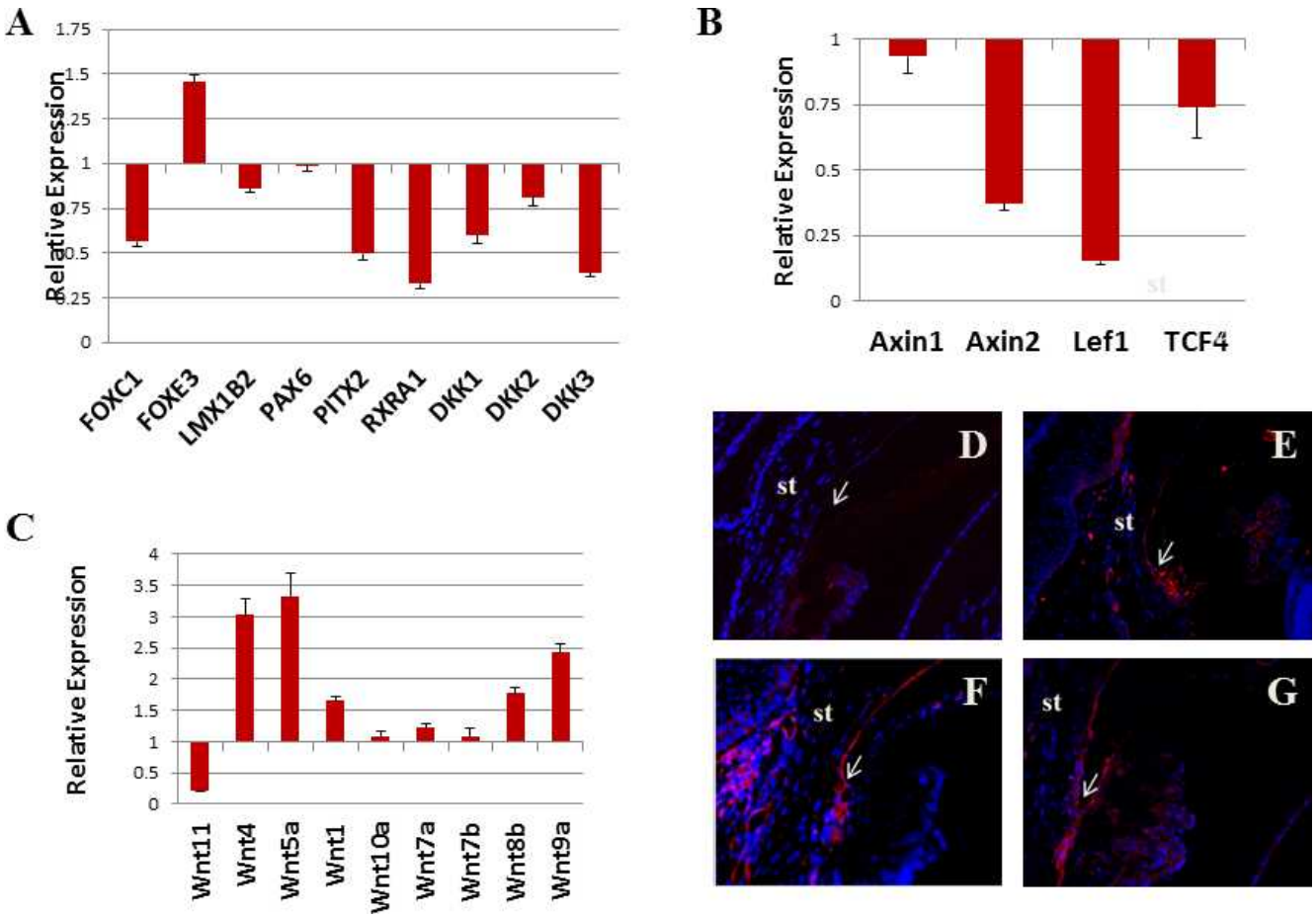

Figure 5. Noncanonical Wnt signal was activated in TGF-α–expressing cornea. Real-time qRT-PCR revealed that *Pitx2*, *RXRα*, and *DKK3* were downregulated more than 2-fold following 10 days of Dox induction compared with uninduced control (**A**). Canonical Wnt targets (*Axin2* and *Lef1*) were also downregulated (**B**). Noncanonical Wnt ligands (Wnt4, Wnt5a, and Wnt9a) were upregulated (**C**). Noncanonical Wnt target, MLC-P, was weakly positive in uninduced corneal endothelium (**D**). Two days after induction, trabecular meshwork and nearby endothelial cells showed stronger signal (**E**). After 5 days of induction, positive cells can be seen in both the trabecular meshwork and corneal endothelium (**F**). After 20 days of induction, positive signal can be seen on both sides of the iridocorneal angle (**G**). st, stroma; *arrows* point to iridocorneal angle.

pathways that activate RhoA/ROCK in pathologic conditions such as ICE or glaucoma. TGF-α is unlikely the direct cause for RhoA activation in our mouse model. We took another approach to address this issue. Reneker et al.[10] found embryonic expression of TGF-α can cause the attachment of iris to the cornea, manifesting as a typical anterior segment defect. In an effort to uncover the underlying mechanism, we analyzed the expression of a panel of genes that have been reported to be critical in anterior segment formation in our adult mice. Among them, *RXRα*, *FoxC1*,[35] *Pixt2*,[36] and *DKK*[17] were downregulated by TGF-α. *RXRα* belongs to the Retinoid X receptor (RXR) family and forms a heterodimer with retinoic acid receptors (RARs). Genetic ablation of *RXRα* in mice results in severe eye defects including anterior segment dysgenesis.[16] *Pixt2* encodes a homeodomain transcription factor that starts expression first in neural crest of the anterior segment at embryonic day (E) 9.5.[36,37] Heterozygous mutations in human *Pitx2* result in Axenfeld-Rieger Syndrome, featuring anterior segment dysmorphogenesis and a high risk for glaucoma.[38] Tissue-specific knockout of *Pitx2* in neural crest recapitulates many ocular features of human mutations, including anterior segment dysgenesis.[37] *FoxC1*, a member of the forkhead family of transcription factors, also plays important roles in ocular morphogenesis.[12] Gage and Zacharias[21] proposed that retinoic acid, *Pitx2*/*FoxC1*, and *DKK*s play a critical role during anterior segment development by suppressing canonical Wnt signaling, so we analyzed the expression of canonical Wnt targets. Because the expression levels of *RXRα*, *Pitx2*, *FoxC1*, and *DKK3* were downregulated in our samples, we expected canonical Wnt signaling targets (*Axin2* and *Lef1*) to be upregulated. To our surprise, they were downregulated. When we looked at the Wnt ligand expression, Wnt4 and Wnt5a, the most abundant Wnt ligands in our sample, were upregulated. They are also the two major noncanonical Wnt ligands.[39,40] The feature of noncanonical Wnt signaling is the activation of RhoA/ROCK signaling and repressing canonical Wnt signaling.[41,42] We demonstrated the upregulation of noncanonical ligands, RhoA/ROCK activation, and downregulation of canonical Wnt targets. All suggested the activation of noncanonical Wnt signaling, thus, noncanonical Wnt signaling is a potential mechanism for RhoA/ROCK activation in affected eyes. More loss-of-function studies, such as knocking down noncanonical Wnt receptor Ror2,[43] are necessary to verify the role of noncanonical Wnt signaling in our mouse model.

In summary, we generated a mouse model that recapitulates some features of ICE syndrome. In this model, anterior segment morphology changes are associated with downregulation of ASD gene expression and the activation of noncanonical Wnt signaling. Currently, we do not know how TGF-α drives the

expression of noncanonical Wnt ligands. We speculate that it may interfere with retinoic acid signaling,[44] triggering a cascade of events that leads to the upregulation of noncanonical Wnt ligands. More studies are needed to investigate the role of retinoic acid and noncanonical Wnt signaling in the pathogenesis of ICE syndrome.

Acknowledgments

The authors thank Mindy Call and Katy Fischesser for proofreading the manuscript.

References

1. De Larco JE, Todaro GJ. Growth factors from murine sarcoma virus-transformed cells. *Proc Natl Acad Sci U S A*. 1978;75:4001–4005.
2. Ciardiello F, Kim N, McGeady ML, et al. Expression of transforming growth factor alpha (TGF alpha) in breast cancer. *Ann Oncol*. 1991;2:169–182.
3. Hise MK, Jacobs SC, Papadimitriou JC, Drachenberg CI. Transforming growth factor-alpha expression in human renal cell carcinoma: TGF-alpha expression in renal cell carcinoma. *Urology*. 1996;47:29–33.
4. Ellis DL, Chow JC, King LE Jr. Detection of urinary TGF-alpha by HPLC and western blot in patients with melanoma. *J Invest Dermatol*. 1990;95:27–30.
5. Rappolee DA, Mark D, Banda MJ, Werb Z. Wound macrophages express TGF-alpha and other growth factors in vivo: analysis by mRNA phenotyping. *Science*. 1988;241:708–712.
6. Luetteke NC, Qiu TH, Peiffer RL, Oliver P, Smithies O, Lee DC. TGF alpha deficiency results in hair follicle and eye abnormalities in targeted and waved-1 mice. *Cell*. 1993;73:263–278.
7. Mann GB, Fowler KJ, Gabriel A, Nice EC, Williams RL, Dunn AR. Mice with a null mutation of the TGF alpha gene have abnormal skin architecture, wavy hair, and curly whiskers and often develop corneal inflammation. *Cell*. 1993;73:249–261.
8. Tuominen IS, Tervo TM, Teppo AM, Valle TU, Grönhagen-Riska C, Vesaluoma MH. Human tear fluid PDGF-BB, TNF-alpha and TGF-beta1 vs corneal haze and regeneration of corneal epithelium and subbasal nerve plexus after PRK. *Exp Eye Res*. 2001;72:631–641.
9. Reneker LW, Silversides DW, Patel K, Overbeek PA. TGF alpha can act as a chemoattractant to perioptic mesenchymal cells in developing mouse eyes. *Development*. 1995;121:1669–1680.
10. Reneker LW, Silversides DW, Xu L, Overbeek PA. Formation of corneal endothelium is essential for anterior segment development—a transgenic mouse model of anterior segment dysgenesis. *Development*. 2000;127:533–542.
11. Semina EV, Reiter R, Leysens NJ, et al. Cloning and characterization of a novel bicoid-related homeobox transcription factor gene, RIEG, involved in Rieger syndrome. *Nat Genet*. 1996;14:392–399.
12. Mears AJ, Jordan T, Mirzayans F, et al. Mutations of the forkhead/winged-helix gene, FKHL7, in patients with Axenfeld-Rieger anomaly. *Am J Hum Genet*. 1998;63:1316–1328.
13. Semina EV, Brownell I, Mintz-Hittner HA, Murray JC, Jamrich M. Mutations in the human forkhead transcription factor FOXE3 associated with anterior segment ocular dysgenesis and cataracts. *Hum Mol Genet*. 2001;10:231–236.
14. Bakrania P, Efthymiou M, Klein JC, et al. Mutations in BMP4 cause eye, brain, and digit developmental anomalies: overlap between the BMP4 and hedgehog signaling pathways. *Am J Hum Genet*. 2008;82:304–319.
15. Stoilov I, Akarsu AN, Sarfarazi M. Identification of three different truncating mutations in cytochrome P4501B1 (CYP1B1) as the principal cause of primary congenital glaucoma (Buphthalmos) in families linked to the GLC3A locus on chromosome 2p21. *Hum Mol Genet*. 1997;6:641–647.
16. Kastner P, Grondona JN, Mark M, et al. Genetic analysis of RXR alpha developmental function: convergence of RXR and RAR signaling pathways in heart and eye morphogenesis. *Cell*. 1994;78:987–1003.
17. Mukhopadhyay M, Gorivodsky M, Shtrom S, et al. Dkk2 plays an essential role in the corneal fate of the ocular surface epithelium. *Development*. 2006;133:2149–2154.
18. Chikama T, Hayashi Y, Liu CY, et al. Characterization of tetracycline-inducible bitransgenic Krt12rtTA/+/tet-O-LacZ mice. *Invest Ophthalmol Vis Sci*. 2005;46:1966–1972.
19. Le Cras TD, Hardie WD, Deutsch GH, et al. Transient induction of TGF-alpha disrupts lung morphogenesis, causing pulmonary disease in adulthood. *Am J Physiol Lung Cell Mol Physiol*. 2004;287:L718–L729.
20. Tanihara H, Hangai M, Sawaguchi S, et al. Up-regulation of glial fibrillary acidic protein in the retina of primate eyes with experimental glaucoma. *Arch Ophthalmol*. 1997;115:752–756.
21. Gage PJ, Zacharias AL. Signaling "cross-talk" is integrated by transcription factors in the development of the anterior segment in the eye. *Dev Dyn*. 2009;238:2149–2162.
22. Yan D, Wiesmann M, Rohan M, et al. Elevated expression of axin2 and hnkd mRNA provides evidence that Wnt/beta-catenin signaling is activated in human colon tumors. *Proc Natl Acad Sci U S A*. 2001;98:14973–14978.
23. Hovanes K, Li TW, Munguia JE, et al. Beta-catenin-sensitive isoforms of lymphoid enhancer factor-1 are selectively expressed in colon cancer. *Nat Genet*. 2001;28:53–57.
24. John SW, Smith RS, Savinova OV, et al. Essential iris atrophy, pigment dispersion, and glaucoma in DBA/2J mice. *Invest Ophthalmol Vis Sci*. 1998;39:951–962.
25. Yanoff M. Iridocorneal endothelial syndrome: unification of a disease spectrum. *Surv Ophthalmol*. 1979;24:1–2.
26. Huang W, Fileta JB, Filippopoulos T, Ray A, Dobberfuhl A, Grosskreutz CL. Hsp27 phosphorylation in experimental glaucoma. *Invest Ophthalmol Vis Sci*. 2007;48:4129–4135.
27. Rao PV, Deng P, Sasaki Y, Epstein DL. Regulation of myosin light chain phosphorylation in the trabecular meshwork: role in aqueous humour outflow facility. *Exp Eye Res*. 2005;80:197–206.
28. Thieme H, Nuskovski M, Nass JU, Pleyer U, Strauss O, Wiederholt M. Mediation of calcium-independent contraction in trabecular meshwork through protein kinase C and rho-A. *Invest Ophthalmol Vis Sci*. 2000;41:4240–4246.
29. Eagle RC Jr, Font RL, Yanoff M, Fine BS. Proliferative endotheliopathy with iris abnormalities. The iridocorneal endothelial syndrome. *Arch Ophthalmol*. 1979;97:2104–2111.
30. Senoo T, Obara Y, Joyce NC. EDTA: a promoter of proliferation in human corneal endothelium. *Invest Ophthalmol Vis Sci*. 2000;41:2930–2935.
31. Zhu YT, Chen HC, Chen SY, Tseng SC. Nuclear p120-catenin unlocks mitotic block of contact-inhibited human corneal endothelial monolayers without disrupting adherent junction. *J Cell Sci*. 2012;125:3636–3648.
32. Edward DP, Morales J, Bouhenni RA, et al. Congenital ectropion uvea and mechanisms of glaucoma in neurofibromatosis type 1: new insights. *Ophthalmology*. 2012;119:1485–1494.
33. Ozawa T, Araki N, Yunoue S, et al. The neurofibromatosis type 1 gene product neurofibromin enhances cell motility by regulating actin filament dynamics via the Rho-ROCK-LIMK2-cofilin pathway. *J Biol Chem*. 2005;280:39524–39533.
34. Honjo M, Tanihara H, Inatani M, et al. Effects of rho-associated protein kinase inhibitor Y-27632 on intraocular pressure and outflow facility. *Invest Ophthalmol Vis Sci*. 2001;42:137–144.

35. Panicker SG, Sampath S, Mandal AK, Reddy AB, Ahmed N, Hasnain SE. Novel mutation in FOXC1 wing region causing Axenfeld-Rieger anomaly. *Invest Ophthalmol Vis Sci*. 2002;43:3613–3616.
36. Perveen R, Lloyd IC, Clayton-Smith, et al. Phenotypic variability and asymmetry of Rieger syndrome associated with PITX2 mutations. *Invest Ophthalmol Vis Sci*. 2000;41:2456–2460.
37. Evans AL, Gage PJ. Expression of the homeobox gene Pitx2 in neural crest is required for optic stalk and ocular anterior segment development. *Hum Mol Genet*. 2005;14:3347–3359.
38. Priston M, Kozlowski K, Gill D, et al. Functional analyses of two newly identified PITX2 mutants reveal a novel molecular mechanism for Axenfeld-Rieger syndrome. *Hum Mol Genet*. 2001;10:1631–1638.
39. Maurus D, Heligon C, Burger-Schwarzler A, Brandli AW, Kuhl M. Noncanonical Wnt-4 signaling and EAF2 are required for eye development in Xenopus laevis. *EMBO J*. 2005;24:1181–1191.
40. Liang H, Chen Q, Coles AH, et al. Wnt5a inhibits B cell proliferation and functions as a tumor suppressor in hematopoietic tissue. *Cancer Cell*. 2003;4:349–360.
41. Nemeth MJ, Topol L, Anderson SM, Yang Y, Bodine DM. Wnt5a inhibits canonical Wnt signaling in hematopoietic stem cells and enhances repopulation. *Proc Natl Acad Sci U S A*. 2007;104:15436–15441.
42. Zhu S, Liu L, Korzh V, Gong Z, Low BC. RhoA acts downstream of Wnt5 and Wnt11 to regulate convergence and extension movements by involving effectors Rho kinase and Diaphanous: use of zebrafish as an in vivo model for GTPase signaling. *Cell Signal*. 2006;18:359–372.
43. Nishita M, Yoo SK, Nomachi A, et al. Filopodia formation mediated by receptor tyrosine kinase Ror2 is required for Wnt5a-induced cell migration. *J Cell Biol*. 2006;175:555–562.
44. Macoritto M, Nguyen-Yamamoto L, Huang DC, et al. Phosphorylation of the human retinoid X receptor alpha at serine 260 impairs coactivator(s) recruitment and induces hormone resistance to multiple ligands. *J Biol Chem*. 2008;283:4943–4956.